International Journal of Research Studies in Science, Engineering and Technology
Volume 6, Issue 3, 2019, PP 1-10
ISSN : 2349-476X

Preparation and Characterization of Flutamide Nanocrystals for in Situ Delivery

L.P. Marques[1*], C. Caramano[2], F.B.T. Pessine[1]

[1]*Chemistry Institute, Universidade Estadual de Campinas, Cidade Universitária Zeferino Vaz, Campinas, Brazil.*
[2]*Biology Institute, Universidade Estadual de Campinas, Cidade Universitária Zeferino Vaz, Campinas, Brazil.*

***Corresponding Author:** L.P. Marques, Chemistry Institute, Universidade Estadual de Campinas, Cidade Universitária Zeferino Vaz, Campinas, Brazil. Email: lpaiferm@gmail.com*

ABSTRACT

Nanonization of poorly soluble drugs is a good strategy to improve their aqueous solubility and possibly improve their pharmacological performance through an increase in the drug bioavailability. The objectives of this work were to produce and characterize Flutamide nanocrystals, to incorporate these nanocrystals into a hydrogel and evaluate its release behavior from this matrix. Flutamide nanocrystals were prepared through the anti-solvent precipitation method. An oxidized citrus pectin hydrogel was produced to perform the in situ delivery of the produced nanocrystals. Prepared nanocrystals have an average particle size of 42.09±0.54 nm and a polydispersity index of 0.532±0.001 nm with a squared morphology. The drug nanonization has improved its solubility and the system has shown a controlled dissolution rate over 200 hours assay.When incorporated into the hydrogel matrix, flutamide nanocrystals were released slowly and steadily, maintaining drug concentration in the external medium, showing the formulation great potential for medical purposes.

Keywords: *flutamide, nanocrystal, hydrogel, prostate cancer*

INTRODUCTION

Prostate cancer is one of the most commonly diagnosed cancers [1]. It is the second leading cause of cancer death of men in many countries. In the United States over than 29,000 deaths were expected to happen in 2018 [2] and there were expected over than 68,000 new diagnosed cases of prostate cancer in Brazil in 2018[3]. These numbers showed the magnitude of this problem and the need for new treatment strategies and for improvements on the existent treatments.

Flutamide (FLU), 2-methyl-N-[4-nitro-3-(trifluoromethyl) phenyl] propanamide, is a non-steroidal anti androgen drug prescribed for the treatment of advanced prostate cancer [4]. The administration of this drug is related to liver injury; in fact, some flutamide's reactive metabolites appear to be involved in hepatotoxicity induction [4-8]. Unfortunately, the occurrence of side effects may be responsible for the discontinuation of the treatment, causing some risks to the patient health. It is well known that low solubility of drugs is a huge challenge in the formulation field because of its impact on the drug bioavailability. In this context nanonization strategies can be used to improve solubility and dissolution rate of poorly water-soluble drugs, leading to higher bioavailability [9]. Drug nanocrystals can be defined as crystals that have dimensions lower than 1µm, in the nanometer range [10, 11].

Drug nanocrystals can be prepared using two different approaches: Top-down and Bottom-up technologies [12]. Top-down methodologies involve drug disintegration through high energy methods, such as wet milling, high-pressure homogenization, and microfluidization; the Bottom-up approach is related to methods that create nanocrystals through precipitation of the drug from an organic solvent [13,14]. In this work, we used the bottom-up methodology of Anti-solvent Precipitation [15] in order to obtain flutamide nanocrystals (FLU-NC).

Gels are semisolid materials made of molecules that can self-organize it, through chemical and/or physical interactions, forming a network that retains the solvent. This self-organization occurs due to covalent bonds, hydrogen bonds

and/or electrostatic interactions [16]. Hydrogels can be defined as polymeric materials with the ability to retain a large amount of water or other fluids without dissolving itself [17]. Besides that, the hydrogels flexibility, similar to that of physiological tissues, and ability to swell guaranteed them considerable notoriety as potential biomaterials [18].

In this work, we present a new approach for prostate cancer treatment, through the in situ delivery of FLU-NC incorporated into a hydrogel. The matrix chosen to produce the hydrogel was Citrus Pectin (CP). The term Pectin is used to identify a group of polysaccharides present in plant cell walls; these molecules are involved in physiological processes and are responsible to maintain the integrity and rigidity of plant tissues [19].Pectin is largely used in food industry as gelling and stabilizing agent, and more recently received the scientific community attention as a potential biomaterial for delivery of amino acids, anti-inflammatory drugs, and genes [20-22].

MATERIALS AND METHODS

Materials

Flutamide(FLU, purity ≥99%), Pluronic® F68, Pectin from citrus peel (galacturonic acid ≥74%), Adipic acid dihydrazide (ADH, purity ≥98%), Dialysis tubing cellulose membrane (MWCO 14,000Da) and DMEM medium were purchased from Sigma-Aldrich (St. Louis, MO, USA). Fetal bovine serum (FBS) was purchased from Gibco (Dublin, Ireland). Tween 80 (T80), acetone and ethanol were purchased from Labsynth (São Paulo, Brazil). Sodium periodate was purchased from Vetec Química Fina (Rio de Janeiro, Brazil). Kollisolv® PEG 400 (polyethylene glycol) was kindly donated by BASF (São Paulo, Brazil). Acetonitrile (ACN, HPLC grade) was purchased from Tedia.Ultrapure water was generated by a Synergy® UV Merck-Millipore (Burlington, MA,USA).

Quantification of Flutamide

Reversed-phase high-performance liquid chromatography (RP-HPLC) analysis of FLU was performed on a Waters UPLC ACQUITY system (Milford, MA, USA). A ZORBAX eclipse plus C18 column (4.6x100mm,5µm) Agilent Technologies (Santa Clara, CA,USA) was used. The mobile phase consisted of ACN and water (60:40 (v/v) ACN: water). Samples were run at isocratic flow of 1 mL/min. Separation was performed at 25°C. The UV absorption detection wavelength was 240nm. FLU had a retention time of 3 min and the total run time was 10 min. All the samples were filtered prior analysis using PVDF syringe filters with 0.45µm porous.

Nanocrystals Preparation

FLU-NC were obtained through the anti-solvent precipitation method [15]. The influence of different solvents and surfactants over FLU-NC characteristics was evaluated. FLU was dissolved in ethanol (FLU-NC-1) or acetone (FLU-NC-2), and the drug solution was added to the surfactants solution containing Pluronic® F68 (F68, 0.06%, w/w) and Tween 80 (T80, 0.70%, w/w) to yield a final FLU concentration of 0.06% (w/w).

The solution was homogenized using a high shear homogenizer Ultra Turrax®IKA for 10 min at 18,000 rpm and the solvent was removed through rotatory evaporation. The final product was stored at 4°C.

Nanocrystals Characterization

Particle size and polydispersity index (PDI) analysis were carried out at a 1:5 (v/v) diluted solution of FLU-NC in deionized water. Size and PDI values were evaluated by dynamic light scattering analysis (DLS, Malvern ZetaSizer-Nano ZS). After this innitial characterization, the FLU-NC-1 was chosen to continue the work and its complete characterization was done.

Changes in crystallinity of FLU-NC-1 in comparison with unmodified FLU were evaluated using differential scanning calorimetry analysis (DSC, TA Instruments 2910). Prior the analysis, a sample of FLU-NC-1 was submitted to lyophilization (FTS Systems Lyophilizer) under -82°C for three days.

The formulation individual components, the physical mixture (PM), and the lyophilized FLU-NC-1 were analyzed. Each sample was placed in an aluminum pan and scanned at 10°C/min rate, under argon flow rate of 10mL/min, with scanning temperature range of 25-300°C.

The nanocrystals (FLU-NC-1) surface morphology was analyzed by scanning electron microscopy (SEM, Quanta FEI 250 Scanning Electron Microscope, operating at 20 kV using a SE detector).

Nanocrystals in Vitro Drug Release Assay

In order to evaluate how the nanonization process would affect the drug solubility, *in vitro* drug release assay was performed with FLU-NC-1 and unmodified FLU. The dissolution media used was Tween 80 solution 4% (w/v). Briefly, 10mL of FLU-NC-1 were transferred into the dialysis bag and suspended into 110 mL of dissolution media with constant magnetic stirring. For comparison purposes, an equivalent amount of unmodified FLU, corresponding the same amount of drug in FLU-NC-1 sample, was dispersed in 10mL of deionized water, then transferred into dialysis bag and placed inside 110 mL of dissolution media. During approximately 200 h, samples of 1mL of the external media were withdrawn and immediately replaced with fresh dissolution media. Sink condition was maintained throughout the experiment. The samples were analyzed using RP-HPLC.

Cell Viability (MTT Assay)

A cell line of prostate cancer (PC3, ATCC® CRL-1435™) was selected for this assay. The line was cultured in 96 well plates (Nest), with 100µL of DMEM medium supplemented with 10% FBS and 0.001% Penicillin / Streptomycin. The plates were kept in an incubator with 5% CO_2 at 37°C for 48 h, a period corresponding to cells confluence.

Dissolutions of FLU-NC-1 were performed with DMEM medium to achieve drug final concentrations of 1.0mM, 2.0mM, and 2.5mM. FLU was used as positive control and its diluent Propylene Glycol was used as negative control. The samples were tested at previously mentioned concentrations in triplicate for a period of 24 h exposure.

For cellular viability evaluation, [3-(4,5-dimethylthiazol-2-yl)-2,5-diphenyl tetrazolium bromide] and formazan (MTT) at a concentration of 0.5mg/mL were used. After 3 h incubation, the absorbance at 540nm was spectrophotometrically read on a Hewlett Packard 8452 A microplate reader.

Oxidation of Citrus Pectin

Oxidized citrus pectin (OP) was obtained through periodate oxidation of citrus pectin (CP) as previously reported [23]. Periodate sodium aqueous solution was added to 2% (w/w) CP solution to achieve $NaIO_4$ final concentration of 12.5mM. The reaction was conduced in the dark for 2 h under continuous magnetic stirring, then 140µL of polyethylene glycol 400 were added to interrupt the oxidation and the system remained under stirring for one additional hour. The reaction product was dialyzed for 3 days against deionized water using a dialysis bag and submitted to lyophilization (FTS Systems Lyophilizer) under -82 °C for three days to obtain a cotton-like OP.

Characterization of Oxidized Citrus Pectin

The oxidation reaction product, OP, and the starting material, CP, were characterized through infrared spectroscopy (FTIR, Agilent Technologies Cary 630) at $4cm^{-1}$ resolution, with 16 scans. Briefly, 0.10000 g of KBr was grounded with 0.00144g of OP or CP, pressed into a disk and analyzed. Additionally, differential scanning calorimetry analysis (DSC, TA Instruments 2910) were carried out, each sample was placed in an aluminum pan and scanned at 10 °C/min rate under an argon flow rate of 10 mL/min, with a scanning temperature range of 25-250°C.

The Hydroxylamine Hydrochloride Titration Assay [24] was used to determine the OP oxidation degree in relation to CP. Briefly, 0.05g (n=4) of OP or CP was dissolved into 12.5mL of 0.25 M hydroxylamine hydrochloride-methyl orange solution and kept under stirring for 2h, then the solution was titrated with 1.0 M sodium hydroxide solution.

Oxidized Citrus Pectin Hydrogel Preparation

The OP-hydrogel network formation occurs due to the establishment of hydrazone bonds between the aldehyde groups of OP and hydrazide groups present on adipic acid dihydrazide (ADH) molecules [23].

Gelification tests were done using a phosphate-saline buffer, pH6.8, and a citrate buffer, pH3.0. In order to maximize the network duration time, different proportions between OP and ADH were investigated and the time from gelification until network collapse was recorded. The ADH concentration was varied from 9.0 to 117.6mM and the OP concentration was varied from 0.4 to 4.2% (w/w). The best formulation was chosen to proceed with the incorporation of flutamide nanocrystals (FLU-NC-1) into the hydrogel matrix.

In Vitro OP-Hydrogel Dissolution Assay

The hydrogel dissolution rate was evaluated by monitoring the hydrogel mass loss over time [25]. The OP-hydrogel *in vitro* dissolution profile was first investigated using two different

dissolution media: phosphate-saline buffer, pH6.8, and citrate buffer, pH 3.0.

To evaluate nanocrystals influence over OP-hydrogel behavior, another dissolution assay was done using OP-hydrogel gelificated with FLU-NC-1 formulation and, for comparison purposes, with a placebo sample composed by OP-hydrogel gelificated in the presence of a surfactant solution. Both assays were done using a phosphate-saline buffer, pH6.8, as dissolution media.

Briefly, 1000µL of OP-hydrogel sample were transferred to a weighted vial and incubated at 37°C for 10 minutes, then 1000µL of dissolution media were introduced onto its surface. At pre-determined time intervals, the dissolution media was completely withdrawn and the vial mass recorded, then 1000µL of fresh dissolution media were replaced onto hydrogels surface. The dissolution rate was calculated by monitoring the hydrogel weight loss over time and flutamide released was quantified using RP-HPLC.

RESULTS AND DISCUSSION

Nanocrystals Characterization

The anti-solvent precipitation method produced NC with the average particle size of 42.09 nm and PDI 0.532 nm, using ethanol as solvent (FLU-NC-1), and average particle size of 244.6 nm and PDI 0.656 nm, using acetone as solvent (FLU-NC-2). The solvent exchange has changed dramatically the average particles size. The analysis of the FLU-NC size distribution curves (Fig. 1) revealed that both samples have not presented unimodal size distribution, justifying the high values obtained for PDI. But, even in the presence of more than one size population, the FLU-NC-1 presented nanocrystals with a more suitable size distribution for the aimed purpose. Besides that, the FLU-NC-2 size distribution curve presented crystals in the micrometer range. Due to its larger size crystals, the FLU-NC-2 formulation was discarded and the work proceeded with FLU-NC-1 formulation complete characterization. DSC thermograms for all nanocrystals formulation components and FLU-NC-1 formulation were recorded and are presented in Fig. 2. The FLU thermogram showed a sharp endothermic peak at 112.1°C corresponding to drug melting [26]; this peak is absent in FLU-NC-1 thermogram indicating possible drug amorphization during the nanonization process. But one may see that FLU melting peak is also absent in physical mixture thermogram, indicating the occurrence of drug dissolution into surfactants mixture. As a matter of fact, thermograms of Pluronic® F68, physical mixture, and FLU-NC-1 all presented only one endothermic transition each, around 50°C, confirming the dissolution hypothesis.

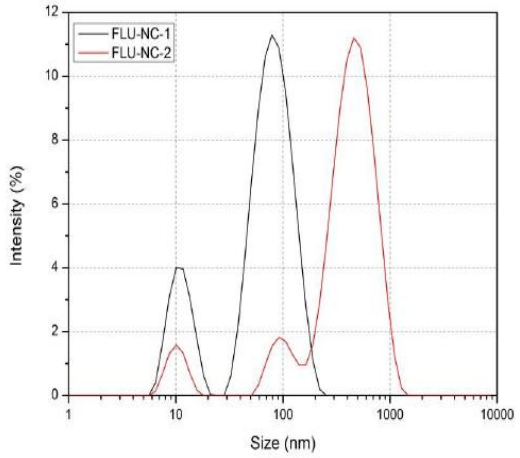

Figure1. *Particle size distribution for flutamide nanocrystals prepared using ethanol (black curve / FLU-NC-1) as solvent, and acetone (red curve / FLU-NC-2) as solvent.*

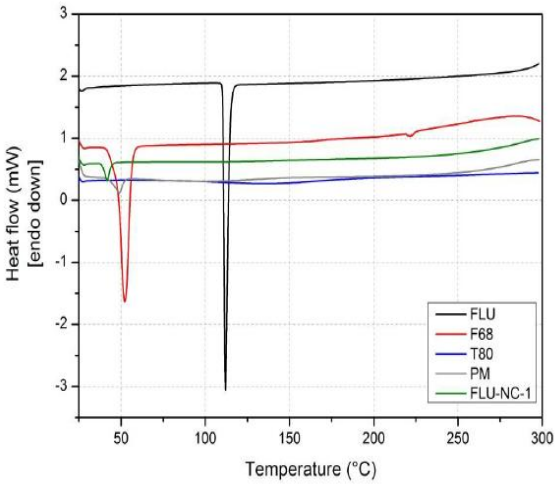

Figure2. *DSC thermograms of flutamide (black curve / FLU), Pluronic® F68 (red curve / F68), Tween 80 (blue curve / T80), physical mixture (purple curve / PM) and lyophilized flutamide nanocrystals (green cruve / FLU-NC-1).*

FLU and FLU-NC-1 surface morphology are shown in Fig. 3. FLU crystals have a classical needle-like shape [26] and the nanonization process changed completely this morphology, as can be seen in Fig. 3b, FLU-NC-1 micrograph presents squared nanocrystals with an individual particle size in the 100 nm to 500 nm range. This result demonstrates the success of the nanonization process. The particle size values obtained with SEM are higher than the values obtained through Zetasizer measurements; this

unconformity can be explained by the nucleation of smaller nanocrystals during samples drying creating bigger nanocrystals prior to the analysis.

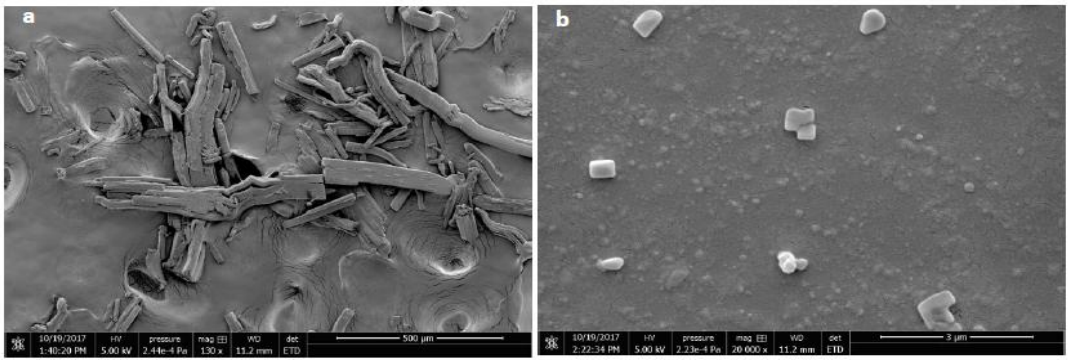

Figure3. *Micrographs of flutamide obtained at a magnification of 130x (a) and FLU-NC-1 obtained at a magnification of 20,000x (b).*

Nanocrystals in Vitro Drug Release Assay

The obtained *in vitro* release profiles are presented in Fig. 4. Flutamide's presence provenient from unmodified FLU dissolution was detectable in external media after 5 h of experiment. In contrast, the drug's presence provenient from FLU-NC-1 dissolution was detectable 30 min, and no burst effect was observed. The drug concentration coming from FLU-NC-1 was maintained at approximately 15% during all 200 h of experiment, showing sustained dissolution profile. The results show a high drug solubility improvement thanks to nanonization process, showing the great potential of this kind of system for medical purposes, once that a poorly water-soluble drug could achieve a significant concentration in solution only a few minutes after its application. Another advantage of nanosuspensions is that there is no drug encapsulation by any structure or polymer, so phenomena as erosion or swelling are not involved in the drug release mechanism [27] and the bioavailability is 100%. Therefore the drug dissolution from nanocrystals occurs through Fickian diffusion. In order to validate this hypothesis, a Zero Order Model was fitted to data obtained from the first 9 h of assay, according to the following equation:

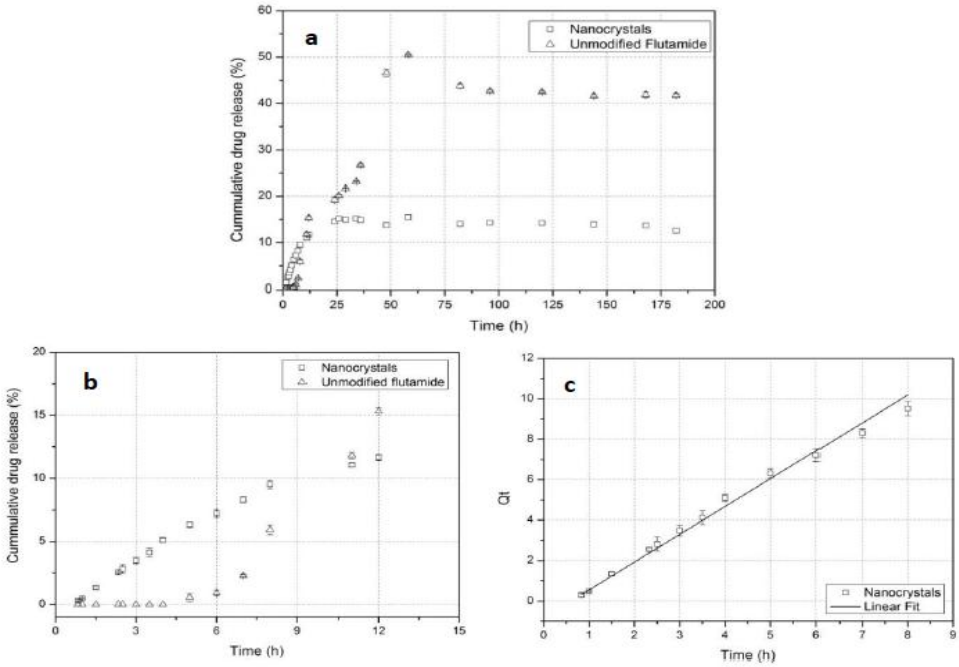

Figure4. *In vitro drugrelease assay results (a), expansion of the first 15 h of the assay (b) and Zero-Order Model fitting (c).*

$$Q_t = Q_0 + k_0 t \qquad (Equation\ 1)$$

where Q_t is the drug amount released in time t, Q_0 is the initial drug amount in the solution and k_0 is the diffusion coefficient. As expected, this model was suitable to describe the experimental data with an obtained Pearson's R value of

0.9965 (Fig. 4c) indicating that nanocrystals dissolution is driven only by the system temperature.

Cell Viability (MTT assay)

The cell viability assay was conducted to evaluate the possibility of flutamide's lost of activity due the nanozitation process. So FLU-NC-1 samples were compared with unmodified FLU dissolved in Propylene Glycol, due the last one's insolubility in aqueous media. Samples incubated with FLU and FLU-NC-1 have shown a significant decrease in number of living cells (about 50% versus control) after 24 h incubation (Fig. 5). This results confirm that the nanonization process did not affected the drug efficacy, showing once again the nanocrystals great potential, once the drug insolubility issue was solved through nanonization. No differences were observed among FLU and FLU-NC-1 concerning relative cell viability related to drug concentration increasing. It seems that a plateau was reached for both samples.

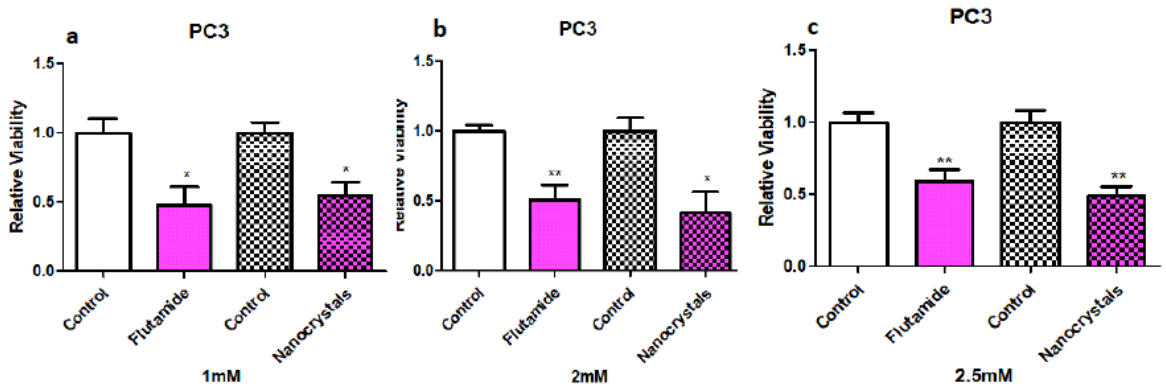

Figure 5. *Cell viability in PC3 cells treated with flutamide and flutamide nanocrystals (FLU-NC-1) at (a) 1mM, (b) 2.0mM and (c) 2.5mM for 24 h. *p≤0.05 Control versus Flutamide or Control versus Nanocrystals. **p≤0.01Control versus Flutamide or Control versus Nanocrystals.*

Oxidized Citrus Pectin Hydrogel Characterization

The chemical structures of CP and OP are fairly similar, since the difference between them is due only to aldehyde groups presence in OP molecule, generated by oxidation reaction (Fig. 6). It is expected, therefore, their absorption spectra in the infrared region to be similar. In addition, the similarity of the spectra may indicate that the oxidation occurred in portions of the PC chain. The carbonyl characteristic infrared bands of aldehyde groups (1740-1720 cm^{-1}), carboxylic acid groups (1700-1680 cm^{-1}) and ester groups (1730-1715 cm^{-1}) occur in regions very close to each other [28,29], making their precise identification a quite challenging.

The spectra obtained (Fig. 7) are quite similar to each other. Both have presented bands in the same regions, making it difficult to confirm the success of the oxidation reaction. The two species present bands in the characteristic region of the stretching band of ester C-O bond; this is due to the fact that CP possesses O-CH_3 groups in substitution of hydroxyl groups of carboxylic acid along its chain; therefore, the spectrum of OP also presents this band. In the obtained spectra there is evidence that 1740 cm^{-1}bands are generated by aldehyde/ester carbonyl groups and 1630 cm^{-1} bands are generated by carbonyl groups of carboxylic acids, indicating the presence of different chemical structures.

The DSC curves obtained for both polysaccharides (Fig 8.) presented quite similar profiles, one endothermic transition, due to polysaccharides melting, followed by an exothermic transition due to their degradation. One may see that the temperatures due to these transitions are different from each other, for CP the melting occurs at 156°C and its degradation takes place at 226°C, but and OP melts at 150°C and degradates at 212°C. These differences indicate the presence of different chemical structures, corroborating the infrared results.

Hydroxylamine hydrochloride reacts with functional groups aldehyde present in OP molecule, forming polioximes and releasing hydrochloric acid equivalents. Then, the degree of OP oxidation can be calculated using the equation:

$$\%Ox = \frac{(nHCl_{OP} - nHCl_{CP})}{nHCl_{OP}} \; x\,100 \quad Equation\ 2$$

where $\%Ox$ is the OP oxidation degree, $nHCl_{OP}$ and $nHCl_{CP}$ are the number of mols of hydrochloric acid generated by hydroxylamine

hydrochloride reaction with oxidized citrus pectin and citrus pectin, respectively.

Through this equation, OP was found to be 70±6% more oxidized than CP, together with FTIR and DSC results it was possible to confirm the success of the oxidation reaction.

Finally, there was observed the OP gelification in the presence of ADH for both pH conditions evaluated (pH 6.8 and 3.0). But for pH 6.8 the network collapsed after less than 1 h of gelification. This pH-effect is related to the nonenzymatic degradation, through β-elimination, that takes place with pectins in which the reaction rate is accelerated with increasing temperature and pH [30]. So, the more acidic condition was fixed, and by varying the proportion between OP and ADH was possible to improve the hydrogel duration time from some minutes to over than 70 h at pH 3.0. The network duration time was found to be related to the ADH amount, high ADH proportions led to short hydrogel duration time. The best condition was found for the sample prepared with 4.2% of the OP and 8.99 mM of ADH in citrate buffer pH3.0 (Fig. 9).

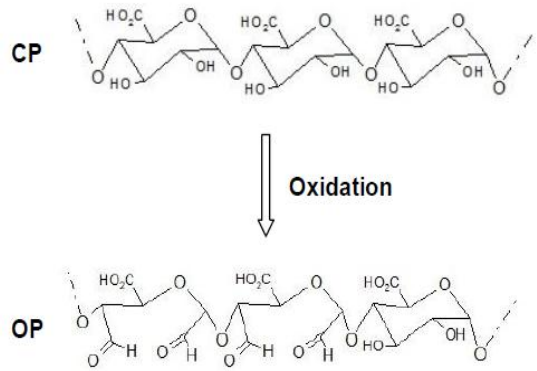

Figure6. *Citrus pectin (CP) oxidation reaction to oxidized citrus pectin (OP).*

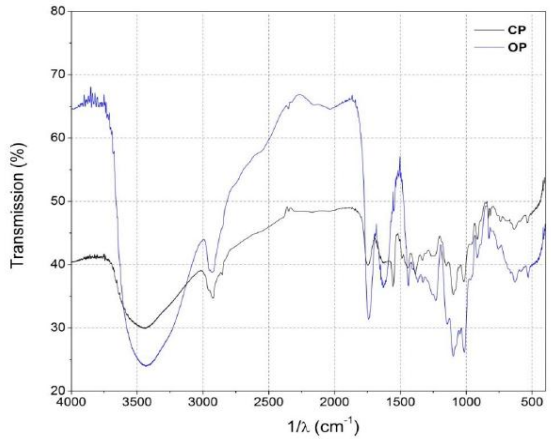

Figure7. *FTIR spectra of citrus pectin (curve in black / CP) and oxidized citrus pectin (curve in blue / OP).*

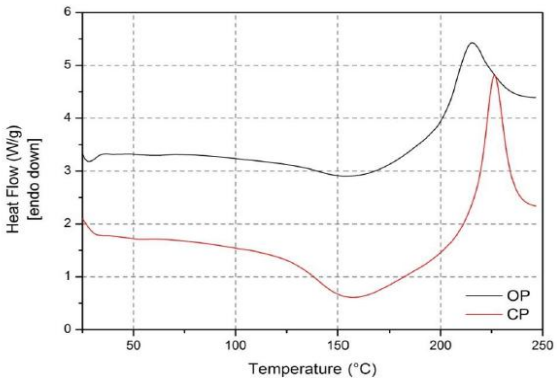

Figure8. *DSC thermograms of citrus pectin (red curve / CP) and oxidized citrus pectin (black curve / OP).*

Figure 9. *Images of oxidized citrus pectin hydrogel gelification in the presence of adipic acid dihydrazide, at pH 3.0.*

In Vitro OP-Hydrogeldissolution Assay

The OP-hydrogel dissolution assay revealed a two phases profile.

First, the hydrogel absorbs the media (swelling phase) and then it starts to lose weight until the hydrogel network collapse (Fig 10). Interestingly, this behavior was observed for both dissolution media (phosphate-saline buffer pH6.8 and citrate buffer pH3.0) meaning that the hydrogel network resistance is more related to its ability to absorb water then it is with the external media pH. Regardless of the dissolution media, all samples have collapsed after 660 min. For the assay conducted using citrate buffer as dissolution media, the hydrogel presented swelling phase of 120 min with a weight increase of 20%. Whereas for phosphate-saline buffer the swelling phase lasted 150 min with 22% weight increase. Then, the weight loss phase has begun with a loss rate of 0.22%/min. at pH 6.8 and of 0.18%/min at pH3.0. Once these values have shown great similarity, the hydrogel dissolution assay in the presence of nanocrystals was done using only phosphate-

saline buffer pH6.8 as dissolution media, due to its physiological relevance.

In the presence of flutamide nanocrystals and placebo (Fig. 11), the OP-hydrogel dissolution behavior was quite different from the previously observed one. An swelling phase lasting 300 min was observed followed by a weight loss phase until the network collapse after 420 min, achieving a total weight loss of only 20%. The interactions between the chemical chains inside the hydrogel matrix were completely modified by the insertion of drug and surfactants (FLU-NC-1) and for the insertion of only surfactants (placebo). The hydrogel had lost its ability to accommodate all the solvent absorbed during the swelling phase and rapidly collapsed after the weight gain. The matrix has become less expandable due to the interactions among polysaccharide chains, flutamide, and surfactants leading to a slower swelling phase.

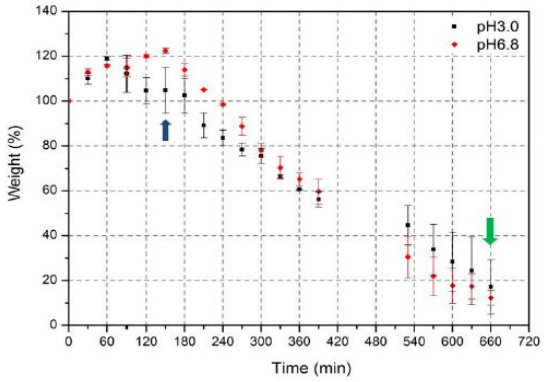

Figure10. *OP-hydrogel dissolution assay in phosphate-saline buffer, pH 6.8 (red curve) and in citrate buffer, pH3.0 (black curve). Blue arrow indicates the swelling phase and green arrow indicates the OP-hydrogel collapse.*

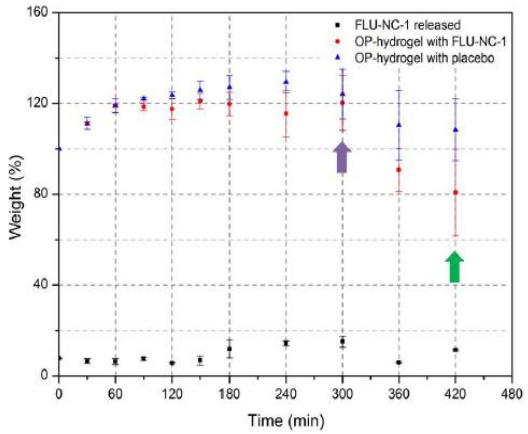

Figure11. *OP-hydrogel dissolution assay in the presence of flutamide nanocrystals (red curve) and placebo solution (blue curve). Flutamide release from OP-hydrogel matrix (black curve). Purple arrow indicates the swelling phase and green arrow indicates the OP-hydrogel collapse.*

Flutamide was quantified in dissolution samples and a slow drug release profile was obtained. As the solvent penetrated the hydrogel network, flutamide nanocrystals were slowly expelled. During the entire assay, flutamide released amount remained below 20% of total releasable drug amount, even when the hydrogel started to lose weight.

The drug was constantly released from the hydrogel matrix, the flutamide concentration was maintained constant over 7 h, confirming the huge potential of the proposed drug delivery system.

CONCLUSION

This study has shown the huge potential that nanocrystals have concerning the improvement of drugs physical-chemical properties. With a simple process was possible to enhance the drug solubility and the MTT results shown that the drug efficacy was maintained.

The flutamide nanocrystals incorporation into a hydrogel matrix has completely changed the last one's dissolution profile; the system hydrogel-nanocrystals slowly released its drug content during 7 hours, with a constant drug-release rate.

Finally, the flutamide nanocrystals utilization could be the key to solving poor solubility problems related to many drugs of interest. Apart that, the purposed system has shown itself as a good alternative for *in situ* delivery of insoluble drugs. The necessity of additional studies concerning the *in vivo* behavior of this system is clear, and the work must proceed to evaluate it.

FUNDING

This research did not receive any specific grant from funding agencies in the public, commercial, or not-for-profit sectors.

REFERENCES

[1] James LJ, Wong G, Craig JC, et al. Men's perspectives of prostate cancer screening: a systematic review of qualitative studies. PLoS ONE. 2017;12(11): e0188258. DOI 10.1371/journal.pone.0188258

[2] Siegel RL, Miller KD, Jemal A. Cancer statistics.2018. CA: Cancer J Clin. 2018;68(1):7-30. DOI 10.3322/caac.21442.

[3] INCA. Estimativa 2018: incidência de câncer no Brasil. Rio de Janeiro [Estimate 2018: incidence of cancer in Brazil. Rio de Janeiro], 2018.

[4] Giorgetti R, Di Muzio M, Giorgetti A, et al. Flutamide-induced hepatotoxicity: ethical and scientific issues. Eur Rev Med Pharmacol Sci.2017;21(1):69-77.

[5] Shet MS, McPhaul M, Fisher CW, et al. Metabolism of the anti androgenic drug (Flutamide) by human CYP1A2. Drug MetabDispos.1997;25 (11):1298-1303.

[6] Ohbuchi M, Miyata M, Nagai D, et al. Role of enzymatic N-hydroxylation and reduction in flutamide metabolite-induced liver toxicity. Drug MetabDispos.2009;37 (1):97-105. DOI 10.1124/dmd.108.021964

[7] Lin AD, Chen KK, Lin AT, et al. Anti androgen- associated hepatotoxicity in the management of advanced prostate cancer. J Chin Med Assoc.2003;66(12):735-740.

[8] Gomez JL, Dupont A, Cusan L, et al. Incidence of liver toxicity associated with the use of flutamide in prostate cancer patients. Am J Med.1992;92(5):465-470. DOI https://doi.org/10.1016/0002-9343(92)90741-S

[9] Kwok PC, Chan HK. Nanotechnology versus other techniques in improving drug dissolution. Curr Pharm Design.2014;20(3):474-482. DOI 10.2174/13816128113199990400

[10] Chen H, Khemtong C, Yang X, et al. Nanonization strategies for poorly water-soluble drugs. Drug Discov Today.2011;16(7–8):354-360. DOI 10.1016/j.drudis.2010.02.009

[11] Junghanns J-UAH, Müller RH. Nanocrystal technology, drug delivery and clinical applications. Int J Nanomedicine. 2008; 3(3):295-310.

[12] Zhang X, Li LC, Mao S. Nanosuspensions of poorly water soluble drugs prepared by top-down technologies. Curr Pharm Design.2014;20(3):388-407.

[13] Lai F, Schlich M, Pireddu R, et al. Production of nanosuspensions as a tool to improve drug bioavailability: focus on topical delivery. Curr Pharm Design.2015;21(42):6089-6103.

[14] Sun B, Yeo Y. Nanocrystals for the parenteral delivery of poorly water-soluble drugs. Curr Opin Solid State Mater Sci.2012;16(6):295-301. DOI 10.1016/j.cossms.2012.10.004

[15] Du J, Li XG, Zhao HX, et al. Nano suspensions of poorly water-soluble drugs prepared by bottom-up technologies. Int J Pharm.2015;495 (2):738-749. DOI 10.1016/j.ijpharm.2015.09.021

[16] Vintiloiu A, Leroux J. Organogels and their use in drug delivery - a review. J Control Release.2008;125(3):179-192.DOI 10.1016/j.jconrel.2007.09.014

[17] Ahmed EM. Hydrogel: preparation, characterization, and applications: a review. J Adv Res.2015;6(2):105-121. DOI https://doi.org/10.1016/j.jare.2013.07.006

[18] Parnes H, Hoque A, Albanes D, et al. Chapter 20 - Prostate Cancer. In: Heber D, Blackburn GL, Go VLW, Milner J. Nutritional Oncology (Second Ed.). Burlington: Academic Press; 2006.

[19] Voragen AJ, Coenen G-J, Verhoef R, et al. Pectin, a versatile polysaccharide present in plant cell walls. Structural Chem.. 2009;20 (2):263-275. DOI https://doi.org/10.1007/s11224-009-9442-z

[20] Liu L, Won YJ, Cooke PH, et al. Pectin/poly(lactide-*co*-glycolide) composite matrices for biomedical applications. Biomaterials.2004;25(16):3201-3210. DOI 10.1016/j.biomaterials.2003.10.036

[21] Opanasopit P, Apirakaramwong A, Ngawhirunpat T, et al. Development and characterization of pectinatemicro / nanoparticles for gene delivery. AAPS Pharm Sci Tech. 2008; 9(1):67-74. DOI 10.1208/s12249-007-9007-7

[22] Jung J, Arnold RD, Wicker L. Pectin and charge modified pectin hydrogel beads as a colon-targeted drug delivery carrier. Coll. Surf B Biointerfaces.2013;104(1):116-121. DOI 10.1016/j.colsurfb.2012.11.042

[23] Takei T, Sato M, Ijima H, et al. *In situ* Gellable Oxidized citrus pectin for localized delivery of anticancer drugs and prevention of homotypic cancer cell aggregation. Biomacromolecules. 2010;11(12):3525-3530. DOI:10.1021/bm1010068

[24] Zhao H, Heindel ND. Determination of degree of substitution of formyl groups in polyaldehyde dextran by the hydroxylamine hydrochloride method. Pharmaceutical Res..1991;8(3):400-402. DOI https://doi.org/10.1023/A:1015866104055

[25] Silveira CP, Apolinário LM, Fávaro WJ, et al. Doxorubicin-functionalized silica nanoparticles incorporated into a thermo reversible hydrogel and intraperitoneally administered result in high prostate antitumor activity and reduced cardiotoxicity of Doxorubicin. ACS Biomaterials Sci Eng..2016;2(7):1190-1199. DOI 10.1021/acsbiomaterials.6b00241

[26] Sternal R, Nugara N. Flutamide. In: Brittain HG. Analytical profiles of drug substances and excipients.Vol 27. New Jersey: Academic Press; 2001, 115-157.

[27] Siepmann J, Siepmann F. Mathematical modeling of drug delivery. Int J Pharm.2008;364(2):328-343. DOI 10.1016/j.ijpharm.2008.09.004

[28] Lopes WA, Fascio M. Flow chart for infrared spectra interpretation of organic compounds. *Quím Nova*. 2004;27 (4)670-673.

DOI http://dx.doi.org/10.1590/S0100-40422004000400025

[29] Gunzler H, Gremlich H. IR Spectroscopy: an introduction. Germany: Wiley-VHC; 2002.

[30] Diaz JV, Anthon GE, Barrett DM. Nonenzymatic degradation of citrus pectin and pectate during prolonged heating: effects of pH, temperature, and degree of methyl sterification. J Agricultural Food Chem.2007; 55(13):5131-5136. DOI 10.1021/jf0701483

Citation: *L.P. Marques, C. Caramano, F.B.T. Pessine." Preparation and Characterization of Flutamide Nanocrystals for in Situ Delivery", International Journal of Research Studies in Science, Engineering and Technology, vol. 6, no. 3, pp. 1-10, 2019.*